

# A Physiologically Based Pharmacokinetic/Pharmacodynamic Model for Carbofuran in Sprague-Dawley Rats Using the Exposure-Related Dose Estimating Model

Xiaofei Zhang,\* Andy M. Tsang,\* Miles S. Okino,<sup>†1</sup> Frederick W. Power,<sup>†</sup> James B. Knaak,<sup>‡</sup>  
Lynda S. Harrison,\* and Curtis C. Dary<sup>†</sup>

\*General Dynamics Information Technology, Henderson, Nevada 89074; <sup>†</sup>National Exposure Research Laboratory, U.S. Environmental Protection Agency (EPA), Las Vegas, Nevada 89193; and <sup>‡</sup>Department of Pharmacology and Toxicology, University at Buffalo, Buffalo, New York 14214

Received April 3, 2007; accepted August 25, 2007

Carbofuran (2,3-dihydro-2,2-dimethyl-7-benzofuranyl-N-methylcarbamate), a broad spectrum N-methyl carbamate insecticide, and its metabolite, 3-hydroxycarbofuran, exert their toxicity by reversibly inhibiting acetylcholinesterase (AChE). To characterize AChE inhibition from carbofuran exposure, a physiologically based pharmacokinetic/pharmacodynamic (PBPK/PD) model was developed in the Exposure-Related Dose Estimating Model (ERDEM) platform for the Sprague-Dawley (SD) rat. Experimental estimates of physiological, biochemical, and physicochemical model parameters were obtained or based on data from the open literature. The PBPK/PD model structure included carbofuran metabolism in the liver to 16 known metabolites, enterohepatic circulation of glucuronic acid conjugates, and excretion in urine and feces. Bolus doses by ingestion of 50  $\mu\text{g}/\text{kg}$  and 0.5 mg/kg carbofuran were simulated for the blood and brain AChE activity. The carbofuran ERDEM simulated a half-life of 5.2 h for urinary clearance, and the experimental AChE activity data were reproduced for the blood and brain. Thirty model parameters were found influential to the model outputs and were chosen for perturbation in Monte Carlo simulations to evaluate the impact of their variability on the model predictions. Results of the simulation runs indicated that the minimum AChE activity in the blood ranged from 29.3 to 79.0% (as 5th and 95th percentiles) of the control level with a mean of 55.9% (standard deviation = 15.1%) compared to an experimental value of 63%. The constructed PBPK/PD model for carbofuran in the SD rat provides a foundation for extrapolating to a human model that can be used for future risk assessment.

**Key Words:** carbofuran; PBPK/PD model; Exposure-Related Dose Estimating Model (ERDEM); Monte Carlo simulation; risk assessment.

**Disclaimer:** The U.S. Environmental Protection Agency through its Office of Research and Development funded and managed the research described here under contract GS-35F-4357D to General Dynamics Information Technology. It has been subjected to Agency review and approved for publication.

<sup>1</sup>To whom correspondence should be addressed at U.S. EPA, Human Exposure and Atmospheric Sciences Division, 944 East Harmon, Las Vegas, Nevada 89193-3478. Fax: (702) 798-2261. E-mail:okino.miles@epamail.epa.gov.

Carbofuran (2,3-dihydro-2,2-dimethyl-7-benzofuranyl-N-methylcarbamate) is a broad spectrum N-methyl carbamate insecticide widely used in agriculture for the control of insects, mites, and nematodes in soil or for fruit, vegetables, and forest crops. Its annual usage in the United States is ~1 million pounds of active ingredient (U.S. EPA, 2006a). Agricultural workers and, to a lesser degree, the general population may be exposed to carbofuran by dermal contact, inhalation, or ingestion as a result of its application for crops or by consuming raw and processed food (U.S. EPA, 2006b).

Carbofuran and its metabolite, 3-hydroxycarbofuran, exert their toxicity by reversibly inhibiting acetylcholinesterase (AChE) (Herzprung *et al.*, 1992; Yu *et al.*, 1972) leading to the persistent action of the otherwise hydrolyzed neurotransmitter, acetylcholine, on its postsynaptic receptors. As mandated by the Food Quality Protection Act (FQPA, 1996), the aggregate exposure and cumulative human health risks need to be evaluated from all pathways of exposure to a class of chemicals acting through a common mechanism of toxicity. The potential health risk of exposure to the N-methyl carbamate insecticides, which exert their toxicity by the same mechanism—AChE inhibition, has been recently assessed (U.S. EPA, 2005, 2006b). All these efforts will benefit from a more systemic understanding of carbofuran's absorption, distribution, metabolism, elimination, and toxicity (ADMET) in mammalian systems. Although previous toxicological studies were performed to quantitatively describe the disposition of carbofuran in mammalian systems (*in vivo* studies: Cambon *et al.*, 1979; Dorough, 1968; Ferguson *et al.*, 1982, 1984; Knaak *et al.*, 1970; Marshall and Dorough, 1979; Metcalf *et al.*, 1968; Padilla *et al.*, 2007; *in vitro* studies: Usmani *et al.*, 2004; Yu *et al.*, 1972), none of the individual study listed could provide a whole picture on carbofuran's ADMET. A pharmacokinetic/pharmacodynamic (PBPK/PD) model for carbofuran, which has not been previously available in the literature for any species, can integrate all the previous study findings into one physiologically based mathematical system. A well-optimized model can be used to predict tissue or blood concentrations of any chemical in the model and AChE activities. More importantly, through interspecies

extrapolation, the rat carbofuran model can serve as a foundation for future human models, which can be further integrated into a human cumulative model to study the cumulative risk of the aggregate exposure of N-methyl carbamate insecticides. Therefore, a PBPK/PD model in the rat for carbofuran is needed. In this study, the tested scenarios focused on oral experiments, which are likely the main route of carbofuran exposure in the general human population (U.S. EPA, 2006b). The study objective was to build an optimized PBPK/PD model for the acute carbofuran oral exposure in the Sprague-Dawley (SD) rat using the Exposure-Related Dose Estimating Model (ERDEM) system through the following procedures: (1) reviewing the literature for potential model parameter values and experimental measurements on carbofuran exposure for the SD rat; (2) optimizing the model parameter values with the experimental measurements; and (3) performing an uncertainty analysis for the model parameters to evaluate the impact of parameter variability.

## MATERIALS AND METHODS

### The ERDEM System

The ERDEM system is a PBPK/PD model construction software developed by Environmental Protection Agency (EPA) (Blancato *et al.*, 2006; U.S. EPA, 2004) for exposure and dose estimation for environmental chemicals. The PBPK/

PD model structure in ERDEM consists of a series of differential mass balance equations describing the ADMET in the physiological compartments of humans and laboratory animals (Blancato *et al.*, 2006; U.S. EPA, 2004). The system enables users to study the exposure and tissue dosimetry relationships and the toxicological risk metrics of interest. Its model engines are written in the Advanced Continuous Simulation Language (ACSL). ERDEM exports particular model specifications which have been input into its graphical user interface (GUI) to an ACSL command file to conduct a PBPK/PD model simulation. In this study, Version 4.1.1 of the ERDEM system (Blancato *et al.*, 2006) was used.

### General Model Structure

Physiological compartments were selected from the available structures in ERDEM to give the model a physiological foundation. The following compartments were included in this study: arterial blood, brain, dermis, fat, gastrointestinal (GI) tract, kidney, liver, rapidly perfused tissue, slowly perfused tissue, static lung, portal blood, and venous blood. In this work, unperfused tissue is not modeled as a separate compartment. The model structure is illustrated in Figure 1. Also indicated in Figure 1 a full GI compartment model, including stomach, duodenum, lower small intestine, and colon, was utilized to describe carbofuran GI absorption, biliary circulation, and fecal elimination. The stomach was considered the major absorption site for carbofuran. Plasma protein binding for any chemical was not included.

### Metabolic Pathways and Urinary Excretion

Chemical structures and molecular weights of carbofuran and its metabolites were found in Knaak *et al.* (2007) and are shown in Table 1. The metabolic pathways in the rat were determined from Ferguson *et al.* (1984), Ivie and Dorough (1968), Knaak *et al.* (1970, 2007), and Metcalf *et al.* (1968) and are shown in Figure 2. All the metabolic reactions were modeled in liver except the

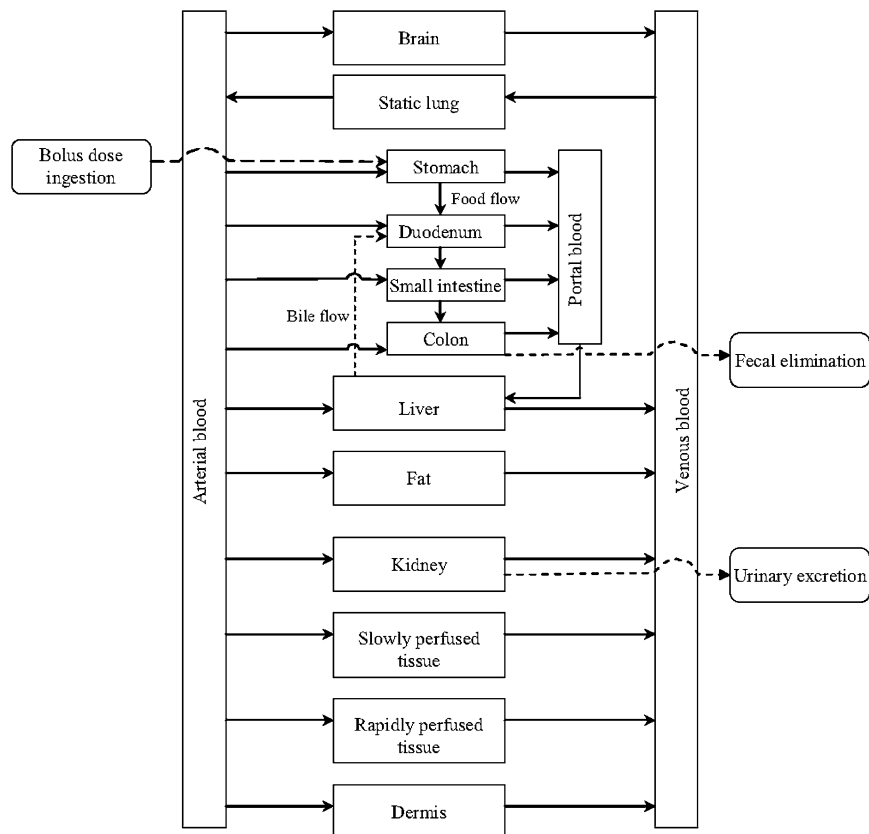


**FIG. 1.** ERDEM PBPK/PD model structure in the rat for the exposure scenario of bolus oral ingestion of carbofuran. A full GI compartment including enterohepatic circulation of glucuronic acid conjugates was implemented.

TABLE 1  
Chemical Information and Structure for Carbofuran and Its Metabolites

Abbreviation <sup>a</sup>	Common name	CAS no.	MW <sup>b</sup>	Structure <sup>c</sup>
CBF	Carbofuran	1563-66-2	221.25	
7PH	Carbofuran-7-phenol	1563-38-8	164.20	
3HOCBF	3-Hydroxycarbofuran	16655-82-6	237.25	
HMCBF	Hydroxymethyl carbofuran	18999-70-7	237.25	
37DI	3-Hydroxycarbofuran-3,7-diol	17781-15-6	180.20	
3KCBF	3-Keto carbofuran	16709-30-1	235.24	
3K7PH	3-Keto-7-phenol	17781-16-7	178.18	
7PHS	7-Phenyl sulfuric acid	70988-92-0	244.27	
7PHG	7-Phenyl glucuronic acid	70988-91-9	340.33	
3HOCBFS	3-Hydroxycarbofuran sulfuric acid	70988-90-8	317.32	
3HOCBFG	3-Hydroxycarbofuran glucuronic acid	53305-32-1	413.38	
HMCBFS	Hydroxymethyl carbofuran sulfuric acid	NA <sup>d</sup>	317.32	
HMCBFG	Hydroxymethyl carbofuran glucuronic acid	NA	413.38	
37DIS	3,7-Diol sulfuric acid	90433-38-8	260.26	
37DIG	3,7-Diol glucuronic acid	90433-37-7	356.33	
3K7PHS	3-Keto-7-phenyl sulfuric acid	70988-94-2	258.25	
3K7PHG	3-Keto-7-phenol glucuronic acid	70988-93-1	354.31	

<sup>a</sup>Chemical abbreviations used in the tables and figures in this study.

<sup>b</sup>Molecular weight.

<sup>c</sup> R<sub>1</sub>, R<sub>2</sub>, and R<sub>3</sub> are connected at the seventh position of the aromatic ring.

<sup>d</sup>NA = Not available.

hydrolysis of glucuronic acid conjugates. The metabolite, 3-hydroxy-N-hydroxymethyl carbofuran (R<sub>2</sub>-OC(O)NHCH<sub>2</sub>OH, see Table 1 for R<sub>2</sub>) reported by Ivie and Dorough (1968) was not considered in this model because it was not evident in other metabolic studies (Knaak *et al.*, 2007). Carbofuran is metabolized mainly by cytochrome P450 (Usmani *et al.*, 2004), but isoforms of cytochrome P450 were not differentiated in this study. Carbofuran metabolism was described by saturable Michaelis-Menten kinetics using  $V_{max}$  and  $K_m$  as indicated in Equation (1). For flexibility, the urinary excretion of the metabolites was modeled as an active and saturable transport process in the kidney tissue with the kinetic equations. Metabolic and urinary  $V_{max}$  were scaled to the actual rat body weight at the power of 0.70 ( $V_{max} \times \text{body weight}^{0.70}$ ), using 1 l as the reference body volume in ERDEM.

$$V = V_{max} \frac{[S]}{K_m + [S]}, \quad (1)$$

where  $[S]$  represents the substrate concentration and  $V$  is the reaction rate.

#### Enterohepatic Circulation of Glucuronic Acid Conjugates

Glucuronic acid conjugates of the following five metabolites were modeled for the enterohepatic circulation: hydroxymethyl carbofuran, carbofuran-7-phenol, 3-hydroxycarbofuran-3,7-diol, 3-keto-7-phenol, and 3-hydroxycarbofuran. The bile flow transports the chemical to the duodenum lumen. The differential

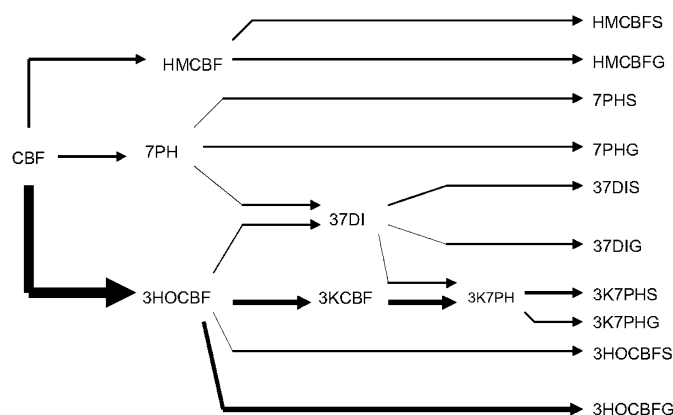


FIG. 2. Metabolic pathways of carbofuran in the rat liver. Chemical abbreviations are indicated in Table 1. Arrow boldness, which was drawn proportionally to the weight of intrinsic clearance ( $V_{max}/K_m$ ) of each reaction, indicates the main and minor reactions. The hydrolysis of glucuronic acid conjugates to their nonconjugate parents, which was depicted by the linear rate constant ( $K$ ), occurred on the duodenum and lower small intestine walls. These reactions are not shown.

equation describing the mass balance of the glucuronic acid conjugates in the duodenum lumen is shown as follows:

$$V_{DUL} \frac{dC_{DULi}}{dt} = Q_{BL,DULi} \frac{C_{LV}}{R_{BL,DULi}} - K_{NL,DULi} A_{DULi} - Q_{F,DUL} C_{DULi}, \quad (2)$$

where  $V_{DUL}$  = volume of duodenum lumen,  $\frac{dC_{DULi}}{dt}$  = the rate of change of the concentration of the  $i$ th glucuronic acid conjugates in the duodenum lumen,  $Q_{BL,DULi}$  = bile flow rate,  $C_{LVi}$  = the concentration of the  $i$ th glucuronic acid conjugates in the liver,  $R_{BL,DULi}$  = bile duodenum partition coefficients for the  $i$ th conjugates,  $K_{NL,DULi}$  = nonlipid flow rate absorption constants for the  $i$ th chemical,  $A_{DULi}$  = amount of the conjugates in the duodenum lumen for the  $i$ th chemical,  $Q_{F,DUL}$  = duodenum food flow rate, and  $C_{DULi}$  = concentration of the  $i$ th conjugates in the duodenum lumen.

The diffusion of the glucuronic acid conjugates from the duodenum and small intestine lumens to the walls was specified by nonlipid flow rate constants. Their breakdown to the parent compound was modeled as occurring on the wall of duodenum and lower small intestine and was depicted by a linear hydrolytic process, which was scaled to the actual rat body weight at the power of 0.25. Both the glucuronic acid conjugates and their parents were modeled to be reabsorbed from the walls to the portal blood by a simple partitioning process. The flow of the enterohepatic circulation is shown in Figure 1. To simulate the bile cannulation test, which withdraws the bile from the bile duct, the reabsorption of related compounds were terminated by setting the nonlipid flow rate constants to zero. The cumulative amounts of the metabolites in the feces were then equivalent to the cumulative biliary excretion.

#### AChE Inhibition in the Blood and Brain

AChE inhibition was modeled in the blood and brain as a bimolecular enzyme inhibition process using the bimolecular inhibition rate constant  $k_i$  (per molar per minute, in ERDEM the actual unit is l/mmol/h). Carbofuran and its metabolite 3-hydroxycarbofuran are known AChE inhibitors (Herzprung *et al.*, 1992). The inhibition process is schematically shown in Figure 3. Although most AChE is associated with the red blood cells (RBCs), the blood was not separated into RBCs and plasma for this PBPK model. The partitioning behavior of carbofuran and its metabolites into the blood components is not known, and to date, concentration measurements have been taken only in whole blood. Therefore, AChE in the whole blood is regarded as one pool of enzyme in this model. Interactions of any chemicals with other enzymes, such as butyrylcholinesterase (BuChE) and carboxylesterase (CaE), were not considered due to very limited information and more incurred uncertainties if they were considered in the model. Range-finding simulations were performed incorporating estimated enzyme levels, and these did not show observable differences in the simulated dose metrics.

#### Experimental Data for Model Parameter Optimization

Three publications on carbofuran oral exposure studies in the SD rat were identified where  $^{14}\text{C}$ -labeled carbofuran was used (Dorough, 1968; Ferguson *et al.*, 1984; Marshall and Dorough, 1979). Marshall and Dorough (1979) reported urinary and biliary cannulation excretion of  $^{14}\text{C}$ -labeled metabolites. The excretion data provide a constraint on the relative amount of chemical that goes through possible metabolism and excretion pathways. The tissue time course data provide constraints on the time scales of absorption and metabolism.

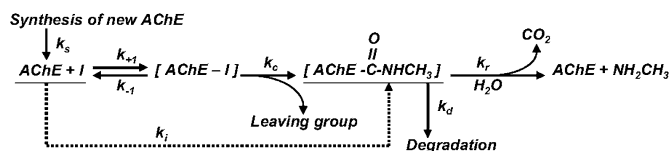


**FIG. 3.** AChE inhibition by carbofuran and its metabolite, 3-hydroxycarbofuran. I: inhibitor (CBF or 3HOCBF).  $k_s$ : resynthesis rate constant of enzyme.  $k_d$ : degradation rate constant of the inhibited enzyme.  $k_r$ : regeneration rate constant of the inhibited enzyme.  $k_i$ : enzyme inhibition rate constant. Leaving group is 7PH for CBF or 37DI for 3HOCBF.  $k_{+1}$ ,  $k_{-1}$ , and  $k_c$  were not modeled.

Carbonyl- $^{14}\text{C}$ -labeled carbofuran enables tracking of metabolites with the intact carbamic bond, but the carbofuran hydrolytic products, which lose this bond, cannot be tracked. Ring- $^{14}\text{C}$ -labeled carbofuran is able to track both groups of chemicals (all metabolites plus carbofuran). Only in Ferguson *et al.* (1984) tissue time concentration data were reported; the radioactivity (DPM per gram of tissue) was converted to mmol/l for ERDEM. The red blood cell (RBC) AChE activity was found in Ferguson *et al.* (1984) as the absolute activity in the unit of  $\mu\text{M ACh/min/ml RBC}$ . To utilize these data for optimizing  $k_i$  values, the absolute AChE activity was converted into the activity in percentage by dividing the AChE activity at control level. Cambon *et al.* (1979) and Padilla *et al.* (2007) also reported AChE and cholinesterase (ChE) inhibition, respectively, but these data were not used for  $k_i$  optimization because of different experimental rats strains used and no measured tissue concentrations. When the experimental data values from the publications were reported in plots, not tables, the plots were scanned and values on the curve were numerically extracted using the digitizing software DigitizeIt (Version 1.5.7, ShareIt! Inc., Cologne, Germany). The digitized experimental values for AChE activity and tissue concentrations of metabolites are provided in the Supplemental Data.

#### Initial Values for Model Parameters

For PBPK/PD model development, values for the physiological, physicochemical, and biochemical parameters are needed. The rat physiological parameters, including compartment volumes (% body volume), compartment blood flows (% of cardiac output), cardiac output and alveolar ventilation rate, were found in Brown *et al.* (1997), Corley *et al.* (1990), Fisher *et al.* (1991, 1998), and Keys *et al.* (2003). AChE concentrations in blood and brain and the enzyme resynthesis and degradation rates were found in Gearhart *et al.* (1990), Hetnarski and O'Brien (1975), and Okino *et al.* (2005). Stomach volume and bile flow rate were found in Bourne (2004). Values for food flow rates and other lumen volumes of the GI tract were determined based on the best estimate of rat physiology.

The physicochemical model parameters are tissue:blood partition coefficients for various chemicals by compartment. The initial values were calculated using a mechanistic model reported by Poulin and Theil (2002) and were found in Knaak *et al.* (2007) in which log D pH 7.4 values were used. The basis of this approach is that the solubility of a chemical in tissue may be approximated by its additive solubility in lipid and water (Poulin and Krishnan, 1995), where lipid solubility is approximated by the  $K_{ow}$ .

The biochemical parameters refer to the  $V_{max}$  and  $K_m$  of Michaelis-Menten kinetics. Values reported in Knaak *et al.* (2007) for carbofuran metabolism were used as the initial values.  $V_{max}$  and  $K_m$  of urinary excretion were not reported in any literature. To run the test model, however, a nominal default value of 0.01 was initially assigned to both  $V_{max}$  and  $K_m$ . The initial set of model parameter values was entered into the ERDEM system via the GUI to establish a testing model for the rat. Except for the physiological parameters, all the other model parameter values were subject to change when necessary in the model optimization process.

#### Model Parameter Value Optimization

The initial ERDEM model was run for the desired output results against the data from all three oral studies. A visual review of plots, observing the level of difference between the ERDEM-simulated output and the experimental data, determined if adjustments in model parameter values would be considered for the next run. This optimization process was conducted by visual examination only rather than with any statistical measure. The initial model outputs from the test model were close in magnitude to the experimental data; however, the fit was not as good as desired. Then the optimization process continued iteratively until a reasonable visual fit was achieved. This established the baseline parameter values. Adjustments to the predicted partition coefficient values were kept within three times their initially predicted values (Payne and Kenny, 2002; Poulin and Theil, 2000). For optimizing  $V_{max}$  and  $K_m$ , the preference was made for changing  $V_{max}$  rather than  $K_m$ , although changes are equivalent at low concentrations. The bimolecular AChE inhibition constants ( $k_i$ ) for the two inhibitors were optimized to fit the RBC AChE activity data (Ferguson *et al.*, 1984) after the two inhibitors' blood concentrations were simulated successfully. A single set of baseline parameter values were able to reasonably simulate the data from the different experiments.

### Model Validation and Application

Ferguson *et al.* (1984) also examined the intravenous injection of carbofuran and the RBC AChE activity, and the tissue concentration data were used for validating the baseline model parameter values in the SD rat. This effort separates aspects of chemical distribution, metabolism, excretion, and enzyme activity from GI absorption because of the directly intravenous delivery of the exposed chemical into the blood.

Since experimental measurements for brain AChE activity in the SD rat were limited, the ERDEM model was run to simulate the total ChE (AChE + BuChE) data reported in Padilla *et al.* (2007) in which 0.5 mg/kg carbofuran was orally administered to Long Evans rats and the time history of ChE activity in RBC and brain was reported. Even though the animal strain was different in the two studies, the ERDEM model was initially run without any change of model parameter values but the body weight of the Long Evans rat and the dose. Model-simulated time history of AChE activity was compared with the Padilla *et al.* (2007) ChE data in RBC and the brain. Separately, the probabilistic distribution of brain AChE activity by the baseline model under the Ferguson *et al.* (1984) scenario was also estimated in subsequent Monte Carlo simulations where all possible variations in the model parameter values were considered simultaneously. For SD rats, the blood inhibition parameters and calculated partition coefficients were used without adjustment.

### Uncertainty Analysis of Model Parameters

Modeling a physiological process involves various uncertainties due to the lack of information or knowledge. Although the data sets described in Experimental Data for Model Parameter Optimization provide some constraints, identification of every parameter value from *in vivo* data is not a realistic expectation for any PBPK/PD model. An uncertainty analysis of model parameters can investigate the impacts on the model output results. The uncertainty for the model parameter values was examined in this study by two related procedures: model parameter sensitivity analysis and Monte Carlo simulations of the model using the oral exposure scenario in Ferguson *et al.* (1984).

**Model parameter sensitivity analysis.** Sensitivity analysis helps identify those model parameters that are most likely to influence the model output results or dose metrics. In this study, a distribution-based relative sensitivity ratio was used to screen the candidate model parameters by observing how changes in a model parameter's value would impact the model's output results. The distribution-based relative sensitivity ratio is based on an algorithm  $(\Delta y/y)/(\Delta x/x)$ , where  $x$  is the baseline value for each model parameter and  $\Delta x$  is the difference between the baseline value and a boundary value. In this study, two boundary values of a model parameter were determined from the probabilistic distribution of its value, that is, first a lower boundary value that represents the 5th percentile and then an upper value which is the 95th percentile value. The 5th and the 95th percentiles will cover the 90% probabilistic interval. The probabilistic distribution of a model parameter value is either a normal or lognormal distribution as appropriate for each model parameter. The  $\Delta y$  is derived from the difference between the baseline model output ( $y$ ) and the model run in which only one particular parameter's value is perturbed with one of its boundary values. This will create two ratio values for each parameter, each from the 5th and 95th boundary value perturbations. An assumption made in the sensitivity analysis was that all model parameters were independent and allowed to change freely even though some model parameters could have dependencies with other parameters. The results of this analysis were used to identify parameters that had a relative sensitivity ratio above a certain level.

**Probabilistic intervals for the selected model parameters.** There are about 300 model parameters in total for the baseline rat ERDEM model. Since many model parameters were included only for consistency with a physiologic description, not all parameters were expected to influence the dose metrics of interest. Based on the experience during the model optimization process, a subset of 109 model parameters was selected for the sensitivity analysis. In this study, all the physiological model parameters, such as body volume, cardiac output, and bile flow rate, were considered to have normal distribution,  $N(\mu, \sigma^2)$  with mean  $\mu$  and standard deviation  $\sigma$ . A 90% probability interval

(the 5th and 95th percentiles) is given by  $\mu \pm z_{0.95}\sigma$ , where  $z_{0.95}$  equals 1.64. The physicochemical and biochemical parameters, such as partition coefficients and  $V_{\max}$ , were considered as skewed parameters with lognormal distribution. For a skewed model parameter  $X$ , the usual monotonic  $W = \log_e(X)$  transform yields a normally distributed variable  $W$  with mean  $\mu_W$  and standard deviation  $\sigma_W$ . The algorithm for the 90% probability range is then the same as for the normal distribution. All the baseline values were used as the average values, that is, estimates of  $\mu$  for the model parameter's probability distribution. A coefficient of variation (CV) for each parameter was then chosen to determine the variation (for normal  $\mu$ ,  $\sigma = (\mu \times CV)$ ). The boundary value algorithm and lognormal transformation for the skewed parameters are shown as follows:

$$\mu_W = \ln\left(\mu_X / \sqrt{1 + CV_X^2}\right) \text{ and } \sigma_W^2 = \ln(1 + CV_X^2), \text{ where } CV_X = \sigma_X / \mu_X$$

is the coefficient of variation. A 90% probability interval for  $W$  is given as  $(\mu_W \pm z_{0.95} \sigma_W)$ .

**Distribution-based relative sensitivity ratio.** A set of model output results or dose metrics was chosen according to the available experimental data of Ferguson *et al.* (1984). To calculate the sensitivity ratio, an output value at a certain time point had to be selected from the time course curve. If there was a peak or trough in the curve, the maximum or minimum value was used. For cumulative metrics, such as mass in urine, the time point comparable to the last observation in the literature was selected to calculate the ratio. To implement the sensitivity analysis, one ACSL command file was created to run the simulation multiple times. For each selected model parameter, a pair of runs would include the upper (95th percentile) value first and then the lower (5th percentile) boundary value while holding the rest of the parameters at their baseline values. Results from the multiple runs were processed by R language routines to select the desired outputs and to calculate the sensitivity ratios for each tested parameter. The parameters with a ratio above a specified level were defined as sensitive and were perturbed in the Monte Carlo simulations.

**Monte Carlo simulations.** To study the impact of the model parameter uncertainty on the model predictions, Monte Carlo simulations were conducted by stochastically and simultaneously varying the sensitive model parameters' values based on their probability distributions. The net effect to the model output could then be investigated in terms of probability distributions. Again, the same oral exposure scenario and outputs in Ferguson *et al.* (1984) were simulated.

**Model parameter distribution specifications.** For the independent and sensitive model parameters, such as body volume, the statistical specifications (distribution and probability interval) used in the Monte Carlo simulations were the same as their specifications in the sensitivity analysis (see the Supplemental Data for the distribution specifications of the sensitive parameters). Compartment volumes and blood flows, however, were treated differently from the sensitivity analysis to take into account the constraint on the total body volume and cardiac output. That is, the values of the nonsensitive compartments for volume and blood flow had to change to follow the change of the sensitive parameters' values. The internal ratios (proportional ratios) among the baseline values of the nonsensitive compartments were maintained. As the largest compartment, slowly perfused tissue was assumed to have a bivariate normal distribution with total body volume (correlation coefficient = 0.80). Another difference from the arbitrarily assigned boundary values in the sensitivity analysis was that a model parameter's range in the Monte Carlo simulations had to reflect the practical and possible values, so the CV was adjusted as needed. The distribution specifications of the compartment volumes and blood flows and their maintenance of mass balance can be found in the Supplemental Data.

**Implementation of Monte Carlo simulations.** For each simulation run, a set of values was generated for all sensitive model parameters by stochastic selection from their probabilistic distributions using the random number generator in the R language. Meanwhile, the nonsensitive parameters were kept at their baseline values. For the Michaelis-Menten kinetic parameters, a  $K_m$  value was always held constant even if it was a sensitive parameter. The corresponding  $V_{\max}$  value was randomly selected instead. An ACSL command file was created so that a set of values for the perturbed parameters could be read in to replace their baseline values. The simulation was aimed to run repeatedly for 10,000 times. The output results were then processed by the R

language to produce simulated percentile curves that described the probabilistic ranges of model outputs. Quality assurance was conducted and both the input of model parameter values for ERDEM and data preparation for uncertainty analysis were reviewed independently to ensure the correctness of input.

## RESULTS

### Baseline Values for Model Parameters

The baseline values determined by the informal optimization process were meant to simulate the average SD rat. The physiological model parameter values for the rat are presented in Table 2. Table 3 shows the parameter values for GI

**TABLE 2**  
Physiological Model Parameter Values for the Rat

Compartment	Compartment volume <sup>a</sup> (%)	Blood flow <sup>a</sup> (%)
Brain	1.21	3.0
Fat	6.00	9.0
Kidney	0.90	17.4
Liver	3.55	20.0
Rapidly perfused tissue	1.24	17.7
Slowly perfused tissue	72.50	15.0
Stomach wall	0.40	1.1
Duodenum wall	0.10	1.0
Lower small intestine wall	1.00	7.4
Colon wall	0.60	1.0
Dermis	5.10	7.4
Arterial blood (AB)	1.75	NA <sup>b</sup>
Venous blood (VB)	3.75	NA
Portal blood (PB)	0.50	NA
Static lung	1.40	NA
Totals	100.00	100.00
	Total body volume	Cardiac output and alveolar ventilation rate
	0.285 (kg) <sup>c</sup>	15.78 (l/h/kg) <sup>d</sup>
	Lumen volume (l) <sup>e</sup>	Food flow rate (l/h) <sup>e</sup>
Stomach	0.0025	0.004
Duodenum	0.0005	0.0032
Lower small intestine	0.003	0.001
Colon	0.002	0.001
Liver	Bile flow from liver to duodenum lumen (l/h)	
	0.001	
	Initial concentration of AChE (mmol/l) <sup>f</sup>	Resynthesis rate for AChE (per hour) <sup>f</sup>
Brain	$3.74 \times 10^{-5}$	0.01
Blood (AB, VB, PB)	$1.10 \times 10^{-6}$	0.01

<sup>a</sup>As % of total body volume and cardiac output for each compartment, respectively. The compartment volume and blood flow were found in Brown *et al.* (1997), Corley *et al.* (1990), Fisher *et al.* (1991, 1998), and Keys *et al.* (2003).

<sup>b</sup>NA = Not applicable.

<sup>c</sup>The average body weight of the SD rats in Ferguson *et al.* (1984) was used.

<sup>d</sup>The listed value is not scaled. ERDEM converts the raw value to the scaled one by the algorithm: Scaled cardiac output =  $15.78 \text{ (l/h/kg)} \times \text{body weight}^{0.74} = 6.233 \text{ (l/h)}$ . Reference body volume = 1 l.

<sup>e</sup>Stomach volume was found in Bourne (2004). The volume of the rest of the GI tract and food flow rates were based on the best estimate of rat physiology.

<sup>f</sup>AChE information was found in Gearhart *et al.* (1990), Hetnarski and O'Brien (1975), and Okino *et al.* (2005).

absorption and the enterohepatic circulation. The physiological GI parameter values in the ERDEM SD rat model were found to be similar with what were reported in Roth *et al.* (1993), such as the bile flow rate, flow rate of feces (in ERDEM it was food flow in colon), and blood flow of the GI tract. The lumen volumes of duodenum, lower small intestine, and colon were derived based on the available knowledge of the rat physiology (Bourne, 2004).

The initial and finalized values for the metabolic reactions and urinary excretion before scaling are shown in Table 4. The major metabolic pathways shown in Figure 2 were configured based on the intrinsic clearance rate (the ratio of  $V_{\max}/K_m$ ) for each reaction, which controls the production of a metabolite when substrate concentration [S] is  $\ll$  than  $K_m$  in Equation (1). Therefore, the ratios of the intrinsic clearance rates among the reactions originated from the same parent chemical decide which reaction as the major or minor reaction. The linear hydrolytic reactions of glucuronic acid conjugates (rate constant  $K$ ) were set to a value of 20 (before scaling) which indicates a fast and complete hydrolytic reaction. Table 5 shows the initial and finalized values of tissue:blood partition coefficients for the 17 chemicals in all compartments.

The bimolecular enzyme inhibition rate constant ( $k_i$ ) values were derived from fitting the RBC AChE activity reported in

**TABLE 3**  
Physiological Model Parameter Values of GI Absorption for the PBPK/PD Model of Oral Exposure to Carbofuran in the Rat

Chemicals <sup>a</sup>	Compartment lumen	Nonlipid flow rate constant (h <sup>-1</sup> ) <sup>b</sup>
CBF	Stomach	3.5
	Duodenum	2.5
	Lower small intestine	2.5
	Colon	No absorption
3HOCBF, HMCBF, 7PH, 37DI, 3K7PH, and their glucuronic acid conjugates <sup>d</sup>	Stomach	NA <sup>c</sup>
	Duodenum	6.0
	Lower small intestine	6.0
Glucuronic acid conjugates	Colon	No absorption
		Bile:duodenum partition coefficient <sup>e</sup>
3HOCBFG		0.0011
HMCBFG		0.004
7PHG		0.03
37DIG		0.01
3K7PHG		0.1

<sup>a</sup>See Table 1 for chemical abbreviations of carbofuran and its metabolites.

<sup>b</sup>This model parameter is a unique feature in ERDEM and describes the movement of the nonlipid component in the GI lumen to the wall while the lipid/chylomicron absorption is described by the lipid flow rate constant.

<sup>c</sup>NA = Not applicable. All the glucuronic acid conjugates and their parents do not appear in the stomach.

<sup>d</sup>All conjugates and their parents were modeled to use the same nonlipid flow rate constant value that was derived from the optimization with the experimental data of Marshall and Dorough (1979).

<sup>e</sup>This model parameter describes the partition process of the glucuronic acid conjugates from bile into the duodenum lumen. The values were derived from the best fit of ERDEM simulated results to the experimental data of Dorough (1968).

TABLE 4  
Biochemical Model Parameter Values for Liver Metabolism and Urinary Excretion

Compartment	Reaction	Metabolic reactions <sup>a,b</sup>	$K_m$ (mmol l <sup>-1</sup> )	$V_{max}$ (mmol l <sup>-1</sup> h <sup>-1</sup> ) <sup>c</sup>		
Liver	Phase I	CBF → 3HOCBF	0.0125 (0.0125) <sup>d</sup>	0.043 (0.0342) <sup>d</sup>		
		CBF → HMCBF	0.02	0.022		
		CBF → 7PH	0.025 (0.0231) <sup>d</sup>	0.021 (0.1372) <sup>d</sup>		
		3HOCBF → 37DI	0.025	0.01		
		3HOCBF → 3KCBF	0.02	0.033		
		7PH → 37DI	0.025	0.0125		
		37DI → 3K7PH	0.02	0.01		
		3KCBF → 3K7PH	0.025	0.04		
		Liver	Phase II	3HOCBF → 3HOCBFS	0.015	0.001
				3HOCBF → 3HOCBFG	0.01	0.015
				HMCBF → HMCBFS	0.015	0.005
				HMCBF → HMCBFG	0.015	0.005
				7PH → 7PHS	0.015	0.007
7PH → 7PHG	0.015			0.005		
37DI → 37DIS	0.015			0.03		
37DI → 37DIG	0.015			0.005		
3K7PH → 3K7PHS	0.015			0.003		
3K7PH → 3K7PHG	0.015			0.0017		
Kidney	Urinary excretion			CBF	0.06	0.01
				7PH	0.4	0.001
				3HOCBF	0.03	0.003
		HMCBF	0.08	0.001		
		37DI	0.1	0.001		
		3KCBF	0.1	0.001		
		3K7PH	0.2	0.001		
		7PHS	0.01	0.002		
		7PHG	0.01	0.002		
		3HOCBFS	0.01	0.008		
		3HOCBFG	0.003	0.009		
		HMCBFS	0.03	0.002		
		HMCBFG	0.03	0.002		
		37DIS	0.03	0.002		
		37DIG	0.03	0.002		
		3K7PHS	0.03	0.002		
		3K7PHG	0.03	0.001		
		Duodenum and small intestine wall	Linear hydrolysis	5 Gs → 5 non-Gs <sup>e</sup>	20 <sup>f</sup>	

<sup>a</sup>See Table 1 for abbreviations used in ERDEM for carbofuran and its metabolites.

<sup>b</sup>The metabolic reactions in liver and urinary excretion are described by Michaelis-Menten kinetics.

<sup>c</sup>The listed values are before scaling. Scaled  $V_{max} = V_{max} \times \text{body weight}^{0.70}$  (reference body volume = 1 l).

<sup>d</sup>The numbers in parentheses were used as initial values (Knaak *et al.*, 2007). Initial values for the other reactions and excretions set  $K_m = 0.01$  and  $V_{max} = 0.01$  (Knaak *et al.*, 2007), since no published values were available. The final parameter values were derived from optimizing the ERDEM baseline model with the experimental data (Dorough, 1968; Ferguson *et al.* 1984; Marshall and Dorough, 1979).

<sup>e</sup>The hydrolysis of glucuronic acid conjugates: 7PHG, 3HOCBFG, HMCBFG, 37DIG, and 3K7PHG to their nonconjugate parents.

<sup>f</sup>The linear rate constant  $K$  is unitless. The listed value is before scaling: Scaled  $K = 20 \times \text{body weight}^{0.25}$ .

Ferguson *et al.* (1984). For carbofuran, the optimized  $k_i$  value was  $2.67 \times 10^6$  per molar per minute, and for 3-hydroxycarbofuran, it was  $1 \times 10^6$  per molar per minute (Table 6). Carbofuran was 2.7 times 3-hydroxycarbofuran on AChE inhibition capability. The products derived from the enzyme inhibition reactions (carbofuran-7-phenol and 3-hydroxycarbofuran-3,7-diol shown in Fig. 3) were not pooled with the metabolic reactions because of their trace production. The first-order regeneration and degradation rate constants of the inhibited enzyme ( $k_r$  and  $k_d$ , respectively) are also shown in Table 6.

#### Model Simulations for Oral Exposure Study 1

Ferguson *et al.* (1984) orally administered SD rats with 50  $\mu\text{g}/\text{kg}$  carbonyl-<sup>14</sup>C-labeled carbofuran. The ERDEM model simulated all the tissue concentration data and cumulative urinary metabolites excretion with reasonable fidelity. Only the time course curves of the simulated blood AChE activity and blood concentration of carbofuran and 3-hydroxycarbofuran are presented here (Figs. 4 and 5). The simulated minimum AChE activity in venous blood occurred at 22 min compared to

TABLE 5  
Tissue:Blood Partition Coefficients for the PBPK/PD Model of Oral Exposure to Carbofuran in the Rat

Chemical <sup>a</sup>	Fat	Brain	Kidney	Liver	Slowly perfused tissue	Dermis	Rapidly perfused tissue, static lung, and GI walls
CBF	4.25 <sup>b</sup>	4.20 [0.6] <sup>c</sup>	2.09 (0.6) <sup>d</sup>	2.15	1.57 (3)	2.47	1.89
7PH	13.57	8.74	3.71	3.96	2.50	4.84	3.23
3HOCBF	0.22	1.08 (1.83) [0.3] <sup>c</sup>	0.98 (0.6)	0.9 (2.3)	0.93 (1.5)	0.84	0.97
HMCBF	0.68	1.55	1.14	1.09 (2)	1.02	1.09	1.11
37DI	0.40	1.28	1.05	0.98	0.97	0.94	1.02
3KCBF	0.54	1.41	1.09	1.04 (2)	1.00	1.01	1.06
3K7PH	2.01	2.66	1.54	1.53	1.25	1.66	1.43
7PHS	0.14	5.33	2.49	2.60	1.80	3.06	2.22
7PHG	0.14	1.02	0.95	0.88	0.91	0.81	0.95
3HOCBFS	0.14	1.18 (0.4)	1.01 (3)	0.94 (3)	0.95 (2)	0.89	0.99
3HOCBFG	0.14	0.98 (0.3)	0.94 (3)	0.86 (3)	0.91 (2)	0.80	0.94
HMCBFS	0.14	10.41	4.30	4.62(6)	2.85	5.70	3.72
HMCBFG	0.14	0.99	0.94	0.87 (2)	0.91	0.79	0.94
37DIS	0.14	1.12	0.99	0.92	0.94	0.86	0.98
37DIG	0.14	0.98	0.94	0.86	0.91	0.79	0.94
3K7PHS	0.14	2.36	1.43	1.41	1.19	1.51	1.34
3K7PHG	0.14	0.99	0.94	0.87	0.91	0.79	0.94

<sup>a</sup>See Table 1 for chemical abbreviations used in ERDEM for carbofuran and its metabolites.

<sup>b</sup>Numbers without parentheses were the initial values derived from the model of Poulin and Theil (2002) as described in Knaak *et al.* (2007) using  $\log D_{pH\ 7.4}$ .

<sup>c</sup>Numbers in square parentheses were the adjusted values used to replace the finalized baseline values in order to fit Padilla *et al.* (2007) enzyme inhibition data in the brain.

<sup>d</sup>Numbers in round parentheses were optimized with the experimental data (Dorough, 1968; Ferguson *et al.*, 1984; Marshall and Dorough, 1979) and used to replace the initial values.

the reported 15 min (Fig. 4), where approximately 40% of the blood enzyme activity was inhibited compared to the reported 37% inhibition. It took 9 min for carbofuran and 3-hydroxycarbofuran (Fig. 5) to reach their blood concentration peaks,  $1.6 \times 10^{-5}$  mmol/l and  $1.49 \times 10^{-5}$  mmol/l, respectively. The peak blood concentrations of the two inhibitors were 14- and 13-fold higher than the AChE concentration in the venous blood ( $1.1 \times 10^{-6}$  mmol/l, Table 2). Therefore, the inhibitor, not the enzyme, dictates the initial degree of AChE inhibition. Therefore, simulating the whole

blood AChE activity can basically represent the RBC AChE activity in the rat, especially when activity is expressed in percentage. The amount of carbofuran excreted through urine without any metabolic change was minor (0.8% of dose at 8 h after exposure compared with the reported 1.4%). The model simulated the cumulative urinary excretion of 3-hydroxycarbofuran glucuronic acid and sulfuric acid as 21.7% of dose compared with the reported 23% at 8 h. For some aspects, the simulated results did not fit completely well with the experimental data. In Figure 5A, the simulated elimination phase of carbofuran

TABLE 6  
Optimized AChE Inhibition Parameter Values for Carbofuran and 3-Hydroxycarbofuran for the Baseline ERDEM PBPK/PD Model and the Model Using the Adjusted Enzyme Inhibition Rate Constants

Pharmacodynamic parameters for AChE inhibition in the rat	Baseline model parameter values <sup>a</sup>	Adjusted parameter values <sup>b</sup>
Enzyme inhibition rate constant ( $k_i$ , per molar per minute)	$2.67 \times 10^6$ (CBF <sup>c</sup> ), $1 \times 10^6$ (3HOCBF <sup>d</sup> )	$4.33 \times 10^5$ (CBF), $1.67 \times 10^5$ (3HOCBF)
Regeneration rate constant of the inhibited enzyme ( $k_r$ , per hour)	2.6	2.6
Degradation rate constant of the inhibited enzyme ( $k_d$ , per hour)	0.001	0.001
Resynthesis rate constant of enzyme ( $k_s$ , per hour)	0.01	0.01

<sup>a</sup>Baseline model parameter values were optimized from Ferguson *et al.* (1984) enzyme activity data.

<sup>b</sup>Baseline model parameter values were adjusted to fit Padilla *et al.* (2007) ChE activity in RBCs and brain after 0.5 mg/kg oral exposure of carbofuran in Long Evans rats.

<sup>c</sup>CBF: Carbofuran.

<sup>d</sup>3HOCBF: 3-Hydroxycarbofuran.



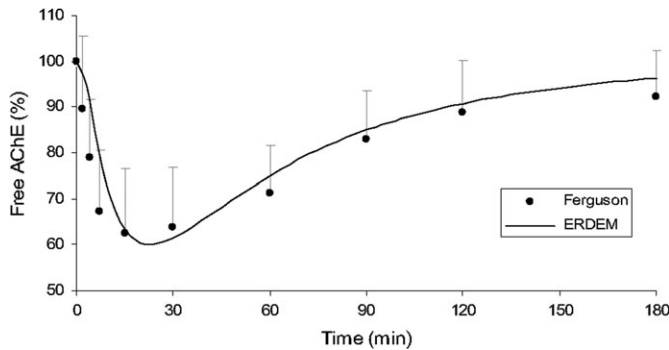


**FIG. 4.** Model simulation for the percentage of free AChE in RBCs after a bolus oral exposure of 50 µg/kg carbofuran in the rat reported in Ferguson *et al.* (1984).

blood concentration was slower than what was indicated by the third experimental observation. Extra measurements around this time point would be helpful for the model construction because this aberrant point was difficult to fit without losing the more important fit of other aspects of the experimental data. The simulated concentration peak of 3-hydroxycarbofuran in blood (Fig. 5B) appeared a little earlier than the experimental peak and was less than the experimental values after 30 min. More experimental data points within 20 min will help to determine when the peak should appear in the time history curve. These results (Fig. 5) were the best available simulations after the parameter optimization process.

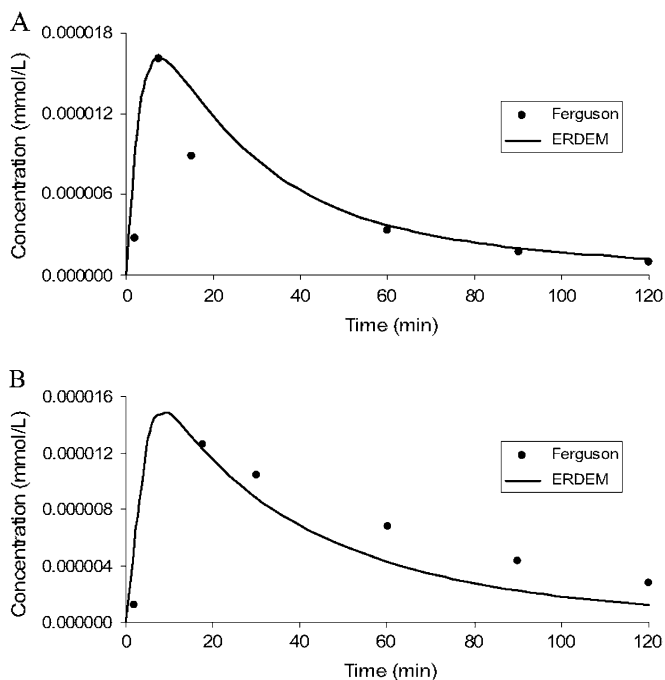


**FIG. 5.** Model simulation for the blood concentration of carbofuran (A) and 3-hydroxycarbofuran (B) after a bolus oral exposure of 50 µg/kg carbofuran in the rat reported in Ferguson *et al.* (1984).

### Model Simulations for Oral Exposure Study 2

In the studies of Dorough (1968), rats were dosed at different levels with carbonyl- and ring-<sup>14</sup>C-labeled carbofuran. Satisfactory fits by visual judgment were seen in the percentage of cumulative excreted dose of total ring chemicals (Fig. 6) and of total carbonyl-labeled chemicals (figure not shown) in urine. Both the ERDEM model-simulated results and the experimental data consistently showed  $\geq 85\%$  of applied dose were excreted in urine after 30 h of exposure. About 40% of the urinary excreted dose was attributed to eight carbamic compounds compared to the experimental value of 38.4%. The ERDEM model suggested that it took 5.2 h for 50% of the applied dose to be excreted in urine (Fig. 6), which was deemed to be the overall half-life of carbofuran oral exposure in the rat. The ERDEM model simulated results also agreed with experimental data in that only a small portion of the applied dose was eliminated in feces, 4.4% from the model simulation compared with the measured 3.3%.

### Model Simulations for Bile Cannulation Test by Oral Exposure

The bile cannulation study (Marshall and Dorough, 1979) used ring-<sup>14</sup>C-labeled carbofuran and provided the valuable information on the production of each metabolite, elimination to urine, and circulation in bile. The experimental measurements constrained the metabolic  $V_{max}$  and  $K_m$  of each metabolite, but the adjustments to the values were limited to maintaining the fit to the blood concentration data for the inhibitors in Ferguson *et al.* (1984). The simulated results of the cumulative percentage of excreted dose for all 17 chemicals in bile and in urine (Fig. 7) fit closely to the experimental measurements. ERDEM model simulation showed that 28.5% of dose was excreted through bile while 67.2% was excreted in urine at 48 h after exposure. This compared consistently to the reported 28.9% in bile and 65.4% in urine. The cumulative biliary and urinary excretion of related metabolites is presented in bar charts (Fig. 8). Nonconjugated chemicals (organosolubles) were modeled in urinary excretion but not in the biliary excretion (presented as zero in Fig. 8A). In urine, the conjugates of 3-hydroxycarbofuran and 3-keto-7-phenol were the most abundant metabolites

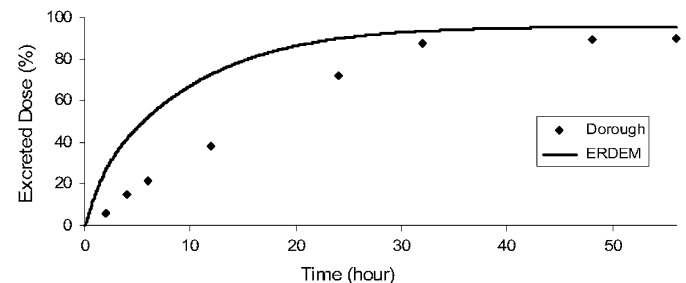


**FIG. 6.** Model simulation for the cumulative percentage of excreted dose of total ring chemicals in urine after a bolus oral exposure of 4.0 mg/kg carbofuran in the rat reported in Dorough (1968).

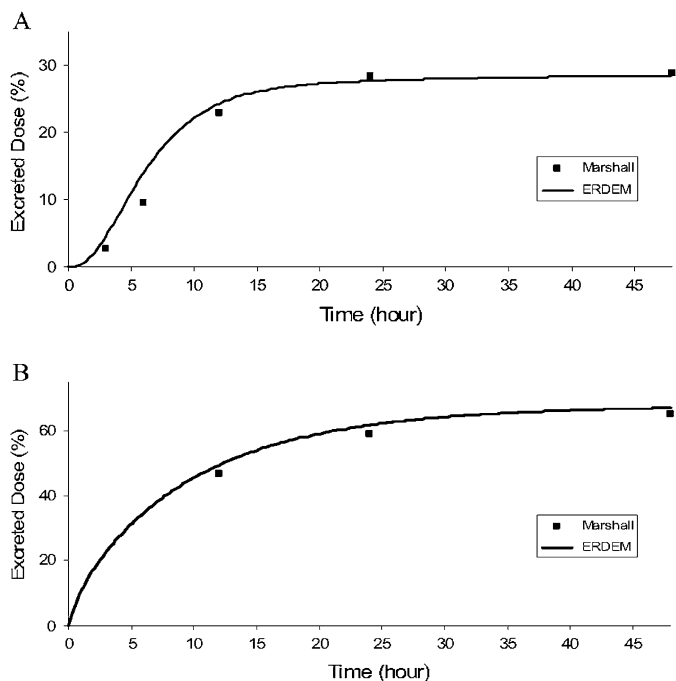


**FIG. 7.** Model simulation for the percentage of cumulative excreted dose for all 17 chemicals in bile (A) and urine (B) after a bolus oral exposure of 0.1 mg/kg carbofuran in the rat bile cannulation test (Marshall and Dorough, 1979).

contributing to 10 and 26.4% of the applied dose (vs. measured 10.3 and 26.7%), respectively (Fig. 8B).

A summary of the ERDEM model simulations against the published data is shown in Table 7. Overall, the baseline model outputs were consistent with the experimental observations.

#### Model Validation and Application

All the experimental data for intravenous injection, which were also reported in Ferguson *et al.* (1984), were simulated with satisfaction. Only the AChE activity and carbofuran concentration in the blood are shown (Fig. 9). The ERDEM model estimated the minimum blood AChE activity as 13% of control level at 3 min after an intravenous injection of 50  $\mu\text{g}/\text{kg}$  carbofuran, compared to the reported 17% at 2 min.

The ERDEM model predicted that brain AChE activity after an oral exposure of 50  $\mu\text{g}/\text{kg}$  carbofuran in the SD rat was inhibited to 30% of the normal level at 24 min as shown by the line labeled as "Mean" in Figure 11B. No AChE activity data in the brain were reported in Ferguson *et al.* (1984). The baseline model used the calculated brain: blood partition coefficients and the same  $k_i$  values for the blood and the brain, that is, the blood AChE inhibition parameters ( $k_{iS}$ ) were used directly for  $k_{iS}$  in the brain because the interaction between AChE and the inhibitors should be independent of enzyme location.

Padilla *et al.* (2007) reported the total ChE activity (AChE + BuChE) in the RBC and brain after oral exposure of 0.5 mg/kg carbofuran in Long Evans rats. The initial simulation of these data was not satisfactory as indicated in Figure 10. Based on

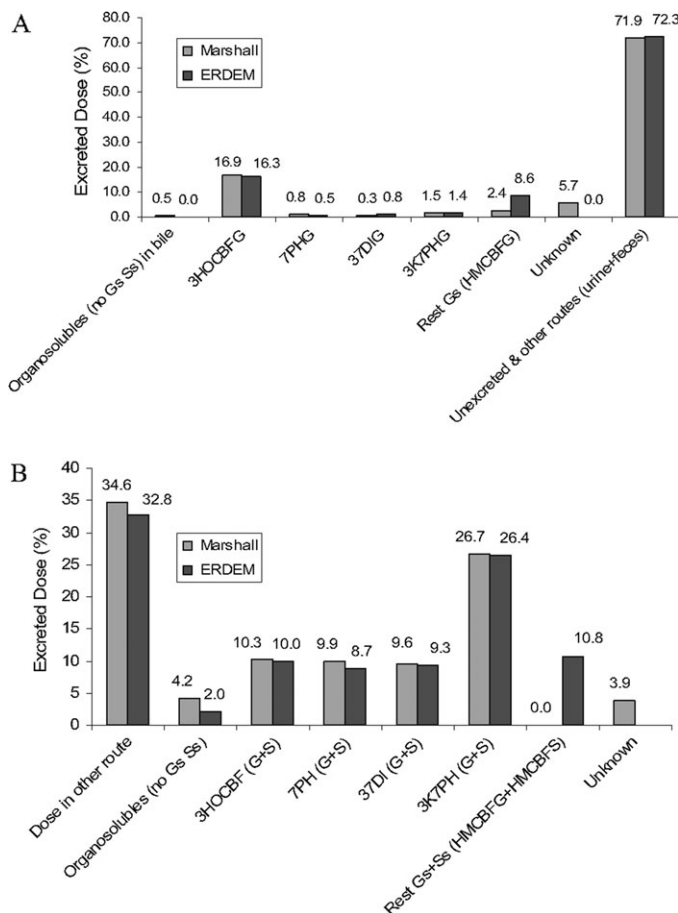


**FIG. 8.** Model simulation for the percentage of cumulative excreted dose of glucuronic acid conjugates in bile at 24 h (A) and that of different metabolites in urine at 48 h (B) after a bolus oral exposure of 0.1 mg/kg carbofuran in the rat bile cannulation test (Marshall and Dorough, 1979). The "unknown" chemicals were not modeled.

the differences, no single set of model parameter values would fit both Padilla *et al.* (2007) and Ferguson *et al.* (1984) blood inhibition data. Therefore, an alternative parameter set was investigated. Adjustment of the metabolic parameter values was not considered since all the tissue concentration and excretion data in Ferguson *et al.* (1984) and Marshall and Dorough (1979) had been simulated well, and no corresponding measurements were reported in Padilla *et al.* (2007). Smaller  $k_i$  values alone (Table 6) could improve the fit of Padilla *et al.* (2007) RBC data, and this inhibition parameter and a lower partition coefficient (Table 5) resulted in fits to the brain data (Fig. 10).

#### Sensitivity Analysis

The scenario in Ferguson *et al.* (1984) was chosen for the sensitivity analysis in order to compare the model predicted output with the experimental measurement in the following Monte Carlo simulations. By using the same toxicological points of interest in Ferguson *et al.* (1984), the sensitivity

TABLE 7  
Comparison of Simulated Results from the ERDEM Baseline PBPK/PD Model of Oral Exposure to Carbofuran in the Rat with Published Experimental Data

Output results	Literature cited	Experimental data	Simulated value
Half-life ( $t_{1/2}$ , h)	EXTOXNET	6–12	5.2
% Applied dose eliminated in feces at 72 h after exposure	Dorough (1968)	3.3	4.4
% Applied dose excreted in urine at 56 h after exposure	Dorough (1968)	89.7	95.5
% Applied dose excreted in bile at 48 h after exposure in the bile cannulation test	Marshall and Dorough (1979)	28.9	28.5
% Applied dose excreted in urine at 48 h after exposure in the bile cannulation test	Marshall and Dorough (1979)	65.4	67.2
Time to the carbofuran blood concentration peak (min)	Ferguson <i>et al.</i> (1984)	8	9
Time to the 3-hydroxycarbofuran blood concentration peak (min)	Ferguson <i>et al.</i> (1984)	17.8	9
Time to the minimum AChE activity in blood (min)	Ferguson <i>et al.</i> (1984)	15	22

analysis indicated how sensitive the model outputs were to the model parameter values and which parameters were being significantly bounded by the Ferguson *et al.* (1984) data. A distribution-based relative sensitivity ratio value of 30% was used as the cutoff for identifying the most sensitive model parameters. The model optimization process provided insights on those parameters that were potentially sensitive. To achieve an overall consistency with this knowledge, three relative sensitivity ratio values (i.e., 5, 30, and 70%) were evaluated. Parameters selected at the 30% cutoff provided a sensitive parameter list which was closest to what had been expected as potentially sensitive ones. Twenty-nine model parameters were found sensitive by this definition for any of the 13 model outputs or dose metrics in Ferguson *et al.* (1984). For one model parameter, blood flow to the brain, the use of its lower limit value produced a ratio of  $-29.03\%$  for AChE activity in the brain. Even though its ratio slightly missed the criterion, it was also included for the consideration of its potential influence on brain enzyme activity. Thus, there were a total of 30 parameters to be perturbed in the Monte Carlo simulations. The sensitive parameters are listed in Table 8, but their ratios for all 13 model outputs are not shown. The influence of some model parameters was universal across all the 13 model outputs or dose metrics. These parameters included body volume, carbofuran stomach absorption (non-lipid flow rate constant), and the  $K_m$  and  $V_{max}$  of the oxidation of carbofuran to 3-hydroxycarbofuran.

#### Monte Carlo Simulation

The Monte Carlo simulations were conducted to analyze the impact of uncertainty of the model parameter values to the model predictions and quantify the current understanding of carbofuran ADMET. The selected probabilistic distribution of the value of each sensitive parameter was either normal such as body volume or lognormal such as the partition coefficients. The distribution represents the possible range of any parameter value centralizing at the average value. When information was limited on the variability of a parameter, a conservative and general rule

was used in determining the CV values and the probability distribution so that a wider range of values could be studied, that is, a medium CVs and lognormal distribution for those parameters with poor information. As a result, the Monte Carlo predictions also showed a wider range (Fig. 11). Special algorithms for the nonsensitive compartment volumes and blood flows were implemented to maintain physiologic consistency. For example, the volume of slowly perfused tissue was found sensitive. When its value was changed in the Monte Carlo simulations, the volume sum of the rest of compartments would also be changed to maintain a sum of 100%. Each of the rest compartments would be assigned from the new residual sum with a new volume under the condition of keeping the same

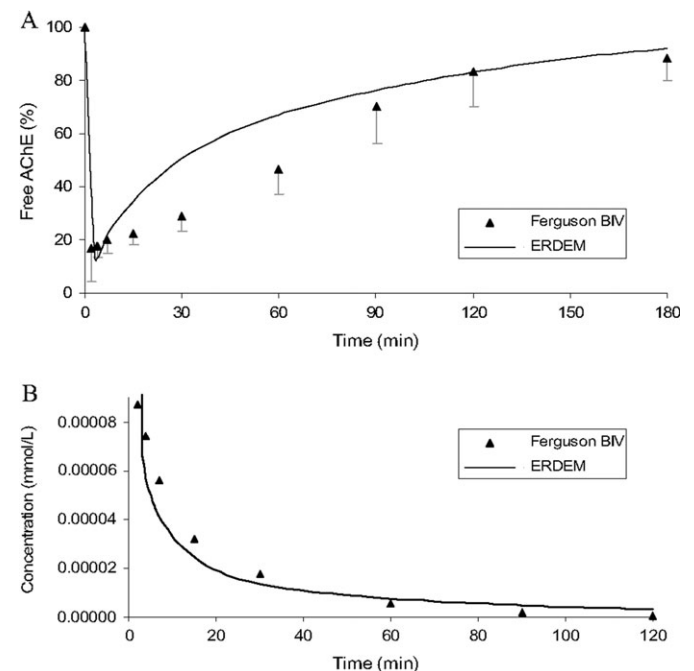
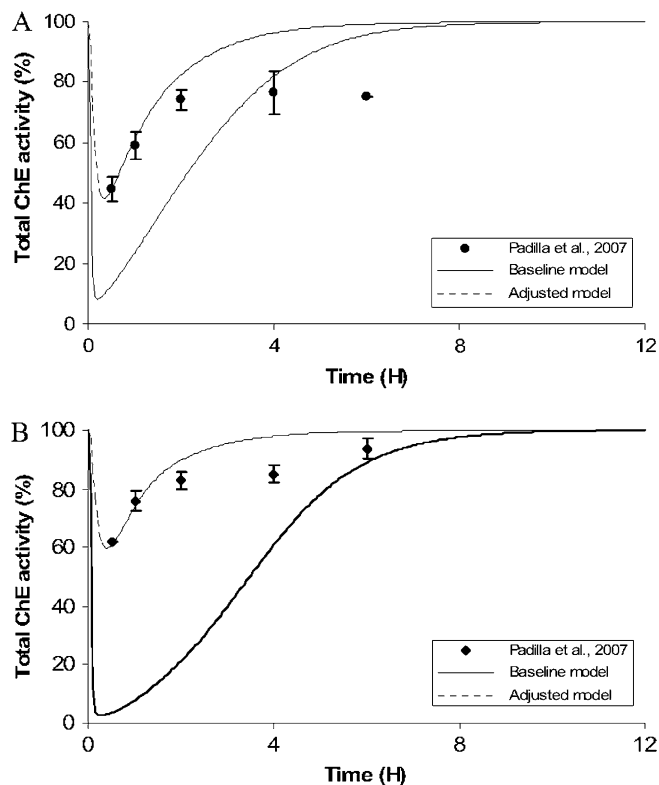


FIG. 9. Model simulation for the percentage of free AChE in RBCs (A) and the blood concentration of carbofuran (B) after a bolus intravenous injection (BIV) of 50  $\mu\text{g}/\text{kg}$  of carbofuran in the rat reported in Ferguson *et al.* (1984).



**FIG. 10.** Simulation of the baseline ERDEM model and the adjusted model (lowered  $k_i$  values plus the reduced partition coefficients for the two inhibitors in the brain) for the total ChE activity after oral exposure of 0.5 mg/kg carbofuran in the Long Evans rats reported in Padilla *et al.* (2007). (A) ChE activity in the RBCs; (B) ChE activity in brain.

ratios of the baseline volume of each of the rest compartments. Ten thousand Monte Carlo simulations were conducted perturbing the 30 sensitive model parameters. Probability distributions of all the 13 output results or dose metrics reported in Ferguson *et al.* (1984) were plotted for review. Only the time course plots of the 5th, 50th (median), and 95th percentiles for AChE activity (%) in blood and brain are shown here in Figure 11. The descriptive statistics and the percentile values for the 13 output results or dose metrics can be found in the Supplemental Data. The simulations indicated that after a single oral exposure to 50  $\mu\text{g}/\text{kg}$  carbofuran in the SD rat, the average of the minimum AChE residual activity in the blood was  $55.9\% \pm 15.1\%$  (mean  $\pm$  standard deviation) of the control level, and the 5th and 95th percentile values were 29.3 and 79.0%, respectively. The average minimum AChE residual activity in the brain was  $32.0\% \pm 16.2\%$  of the control level and its 5th and 95th percentile values were 8.6% and 61.3%, respectively. As shown in Figure 11A, the 5th and 95th percentile band for the blood AChE activity covered the experimental data. Both median and mean curves were also close to the experimental data indicating that the central tendency of the simulated results was statistically consistent with the experimental data. Ninety percent of the simulated curves for AChE activity in blood and brain showed

**TABLE 8**  
List of Sensitive Model Parameters Found by the Sensitivity Analysis for the Carbofuran ERDEM PBPK/PD Model in the SD Rat

Model parameter <sup>a</sup>
Total body volume (l)
Compartment volume (%)
Slowly perfused tissue
Cardiac output (total blood flow)
Compartment blood flow (%)
Brain
Kidney
Liver
Slowly perfused tissue
Bile flow rate
Bile flow rate (l/h)
GI absorption
CBF nonlipid flow rate constant in stomach (per hour)
Partition coefficients
CBF-liver
CBF-kidney
CBF-brain
3HOCBF-liver
3HOCBF-kidney
3HOCBFG-liver
3HOCBFG bile-duodenum
Liver metabolism
$V_{\max}$ (mmol/l/h)
CBF $\rightarrow$ 3HOCBF
3HOCBF $\rightarrow$ 3KCBF
3HOCBF $\rightarrow$ 3HOCBFG
$K_m$ (mmol/l)
CBF $\rightarrow$ 7PH
CBF $\rightarrow$ 3HOCBF
CBF $\rightarrow$ HMCBF
3HOCBF $\rightarrow$ 3KCBF
3HOCBF $\rightarrow$ 3HOCBFG
Urinary elimination <sup>c</sup>
$V_{\max}$ (mmol/l/h)
CBF
3HOCBF
$K_m$ (mmol/l)
CBF
3HOCBF
AChE inhibition in the blood and brain
Enzyme regeneration rate constant (per hour)
CBF enzyme inhibition rate constant (per molar per minute)

<sup>a</sup>See Table 1 for chemical abbreviations. Parameter with a sensitivity ratio over than 30% was regarded as sensitive.

that AChE was inhibited to the minimum level within 30 min after exposure.

## DISCUSSION

In this study, the ERDEM PBPK/PD model for carbofuran was focused on oral exposure in the SD rat using three

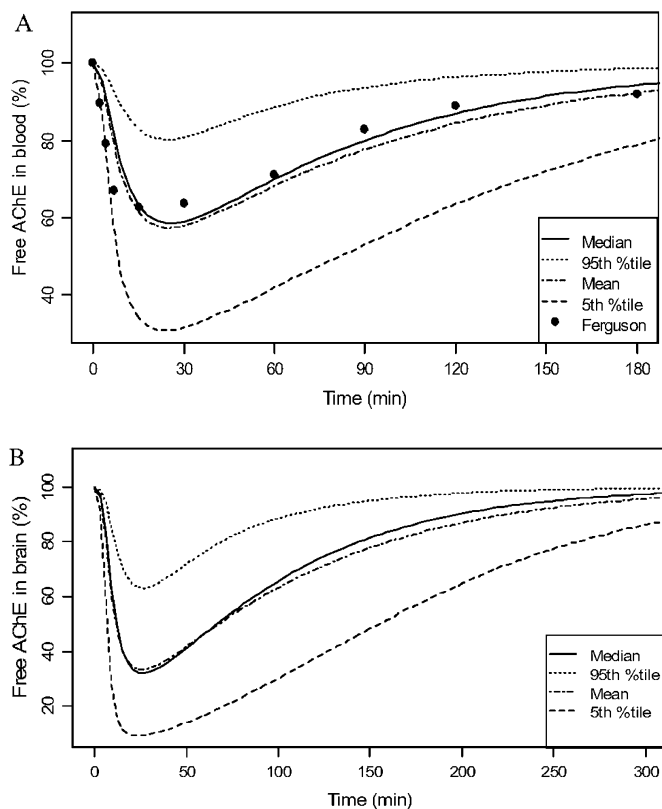


**FIG. 11.** Monte Carlo simulations (ERDEM) for the free AChE in RBCs (%) (A) and in the brain (%) (B) after the bolus oral exposure to carbofuran in the rat reported in Ferguson *et al.* (1984). No experimental data in the brain were available for comparison.

experimental data sets for optimizing the model parameter values. In general, the baseline model described carbofuran's ADMET in the SD rat with reasonable fidelity to the experimental measurements. The study by Marshall and Dorough (1979) provided evidence of the need to include the enterohepatic circulation in the model because of the high percentage (28.9%) of dose excreted in bile. As one of the AChE inhibitors, 3-hydroxycarbofuran and its glucuronic acid conjugate were modeled to participate in this circulation. Therefore, its toxicity was enhanced due to its recycling from the GI tract and the resultant longer residence time. The composition information for each metabolite in bile and urine (Fig. 8) reported in the bile cannulation study (Marshall and Dorough, 1979) was used as the reference to simulate their metabolic production and was the most important evidence to derive the metabolic  $V_{max}$  and  $K_m$  values. Both the experimental data (Dorough, 1968) and the ERDEM model simulation indicated that the major elimination route for carbofuran was urinary excretion, 95.5% of applied dose in urine at 56 h and only 4.4% eliminated in feces at 72 h. Consistent with what was found by Dorough (1968), 3-keto-7-phenol and 3-hydroxycarbofuran conjugates were the main urinary metabolites in the SD rat.

In liver, carbofuran is either oxidized or hydrolyzed, leading to different toxicological effects. Hydrolysis is the detoxification process resulting in the enzyme inhibition capability disabled. Two other enzyme esterases, BuChE and CaE, were not included in the ERDEM model. Since their major function is to hydrolyze the inhibitors thus detoxifying the AChE inhibition, this hydrolytic effect by the two enzymes had been actually included by optimizing the  $V_{max}$  and  $K_m$  values of the hepatic reaction of carbofuran to 7-phenol resulting in the excellent fit to the tissue concentration data of the two inhibitors. So the separate inclusion of these two enzymes is not necessary. A recent *in vitro* study by Usmani *et al.* (2004) showed that the intrinsic clearance rate ( $V_{max}/K_m$ ) of carbofuran oxidation to 3-hydroxycarbofuran by the rat was 16 times that of human thus indicating that humans are not as active as rodents in carbofuran oxidation. This difference should be reflected in any future human model when the rat model is used as a basis for extrapolation.

Carbofuran and 3-hydroxycarbofuran were modeled as the two AChE inhibitors. The bimolecular inhibition rate constant ( $k_i$ ) for carbofuran was reported for bovine RBCs by Yu *et al.* (1972) and  $k_i$ s for both inhibitors in electric eels by Herzsprung *et al.* (1992). Although data were for different species, they provided useful reference for the  $k_i$  values for the rat. The ERDEM baseline model value was 1.57 times the published  $k_i$  for eel, 3.34 times the bovine for carbofuran, 4.86 times the value for eel, and 5.56 times the bovine for 3-hydroxycarbofuran (Herzsprung *et al.*, 1992). The same magnitude between the optimized and the measured  $k_i$ s supports that it is appropriate to use the RBC AChE activity (%) to optimize the toxicodynamic part of the ERDEM model under the situation of limited AChE inhibition data from the literature. The achievement of satisfactory fit of blood concentrations of the two inhibitors plus the mechanistic approach for estimating the partition coefficients (Poulin and Theil, 2002) should enable the model to tentatively predict the brain concentrations of the two inhibitors.

After oral dosing, Padilla *et al.* (2007) reported that total ChE (AChE + BuChE) in the brain was inhibited to a less extent than that in the RBC in Long Evans rats. Without making adjustments from the blood inhibition parameters, the baseline model predicted that AChE in the brain was inhibited to a greater extent than in blood (Fig. 10). Cambon *et al.* (1979) also reported that the brain AChE was inhibited to a more extent than that in the blood in the pregnant SD rats: 69% versus 83% at 0.25 mg/kg and 44% versus 79% at 2.5 mg/kg after 1-h carbofuran oral exposure. The higher levels of brain versus blood inhibition in the baseline model and Cambon *et al.* (1979) do fall within the reported scatter reported in Padilla *et al.* (2007). In both the model simulation and the experimental studies, blood and brain enzyme activities were restored to at least 90% of the normal levels within 5 h after exposure. To simulate the Padilla *et al.* 2007 data, the  $k_i$  values had to be reduced and the brain: blood partition coefficient was

lowered from 4.2 to 0.6 for carbofuran and from 1.08 to 0.3 for 3-hydroxycarbofuran. Such a large change from the calculated partition coefficient values may indicate the involvement of an active transporter across the blood-brain barrier or local metabolism in the brain (Payne and Kenny, 2002; Poulin and Theil, 2000). Currently, data are unavailable to differentiate between the possibilities.

An issue that impacts the PBPK/PD model prediction is that the data sets on RBC enzyme inhibition in rats are not consistent. Ferguson *et al.* (1984) was used for parameter estimation since it is the only study that measured both enzyme inhibition and tissue concentrations represented in a PBPK/PD model. Also, the study used a lower dose, which is desirable for the ultimate purpose of simulating exposure concentrations. The same extent of RBC enzyme inhibition that was seen in Ferguson *et al.* (1984) occurred with a dose that was 10-fold lower than the dose in Padilla *et al.* (2007). The doses and resulting level of enzyme inhibition in Cambon *et al.* (1979) are more consistent with Padilla *et al.* (2007) than the model presented here. Some of the differences could be due to the experimental animals, where Ferguson *et al.* (1984) used adult SD rats, while Cambon *et al.* (1979) used pregnant SD rats and Padilla *et al.* (2007) used Long Evans rats. However, based on the sensitivity analysis, the different response is unlikely to be attributed to only the anatomical differences reported for Long Evans rats in Simmons *et al.* (2002) and pregnant rats in Fisher *et al.* (1989). These differences, as well as the large ranges shown in the uncertainty analysis, indicate that more experimental measurements of both concentrations and AChE activity in the blood or RBC and in the brain in the same rat strain would be valuable. At this point, it would be appropriate to leave the determination of the  $k_i$  value open to the readers whenever more experimental data are available.

Using the same set of model parameter values from the oral exposure scenario to simulate another route of exposure can validate the predictive capabilities of the model. To simulate the intravenous injection, no new model parameters were added to the oral model. The simulated results (Fig. 9) indicated that the model parameter values were still valid for describing intravenous injection scenario. As shown in Table 7, the general model behavior in ERDEM was very close to the corresponding experimental observations. These general aspects were the primary restrictions considered during parameter optimization.

The sensitivity analysis of model parameters was to identify those parameters that would substantially impact the model output results. Therefore, the sensitive parameters should be considered as the priorities for experimental measurement. Of the 30 sensitive model parameters, four could substantially impact the AChE activity in the blood. The enzyme regeneration rate constant ( $k_r$ ) and the enzyme inhibition rate constant ( $k_i$ ) were directly related to AChE activity. The liver: blood partition coefficient for carbofuran determined carbofuran's distribution to the liver where the metabolic

reactions occurred and impacted the blood AChE activity indirectly since blood enzyme activity was determined by the two circulating inhibitors. Body volume determined the total amount of AChE in the blood and the amount of the metabolic enzymes in the liver. Therefore, it also affected the AChE activity in the blood indirectly. Monte Carlo simulations were implemented to examine the possible range of model outputs due to the uncertainty of the parameter values. Thus, the model outputs were no longer deterministic but were presented as probability distributions. As plotted in Figure 11A, the central tendency (baseline and median curves) was close to the experimental values, suggesting that the ERDEM model could replicate the experimental data reasonably.

The carbofuran PBPK/PD model, description of its development, and characterization of its outputs illustrate important areas of additional research on the ADMET of carbofuran. Of particular need are the dynamic parameters associated with enzyme inhibition and metabolism. Because of the lack of human ADMET data for carbofuran, direct construction of a human model would be unreliable. With this optimized rat model available, a human model could potentially be derived by including the human physiological parameters and the human characteristics of less metabolic oxidation. In conclusion, the optimized ERDEM PBPK/PD model for the SD rat was constructed successfully and could reasonably simulate carbofuran's disposition and toxicity. The results of this predictive ERDEM PBPK/PD model and future human model will provide a promising tool for the human risk assessment for carbofuran.

#### SUPPLEMENTARY DATA

Supplementary data are available online at <http://toxsci.oxfordjournals.org>.

#### ACKNOWLEDGMENTS

The authors gratefully acknowledge the help of the following staff of General Dynamics Information Technology in this study: Naser E. Heravi, Jerry J. Lorenz, and Carol B. Thompson. And with great sorrow, our team extends our heartfelt feelings of loss to family and friends of our dear colleague Fredrick W. Power, the architect of the ERDEM modeling platform; a kind and gentle soul. We dedicate this manuscript and others to his memory. "Fred, we could never have done this work without you."

#### REFERENCES

- Blancato, J. N., Power, F. W., Brown, R. N., and Dary, C. C. (2006). *Exposure Related Dose Estimating Model (ERDEM) a Physiologically-Based Pharmacokinetic and Pharmacodynamic (PBPK/PD) Model for Assessing Human Exposure and Risk* U.S. Environmental Protection Agency Washington, DC EPA/600/R-06/061 (NTIS PB2006-114712).
- Bourne, D. W. (2004). Rat physiology on line resource. Available at: <http://www.boomer.org/pkin/PK04/PK2004570.html>. Accessed September 2007.

- Brown, R. P., Delp, M. D., Lindstedt, S. L., Rhomberg, L. R., and Beliles, R. P. (1997). Physiological parameter values for physiologically based pharmacokinetic models. *Toxicol. Ind. Health* **13**, 407–484.
- Cambon, C., Declume, C., and Derache, R. (1979). Effect of the insecticidal carbamate derivatives (carbofuran, pirimicarb, aldicarb) on the activity of acetylcholinesterase in tissues from pregnant rats and fetuses. *Toxicol. Appl. Pharmacol.* **49**, 203–208.
- Corley, R. A., Mendrala, A. L., Smith, F. A., Staats, D. A., Gargas, M. L., Conolly, R. B., Andersen, M. E., and Reitz, R. H. (1990). Development of a physiologically based pharmacokinetic model for chloroform. *Toxicol. Appl. Pharmacol.* **103**, 512–527.
- Dorough, H. W. (1968). Metabolism of furadan (NIA-10242) in rats and houseflies. *J. Agric. Food Chem.* **16**, 319–325.
- EXTOXNET: Oregon State University. *Pesticide Information Profiles: Carbofuran*. Available at: <http://extoxnet.orst.edu/pips/carbofur.htm>. Accessed September 2007.
- Ferguson, P. W., Dey, M. S., Jewell, S. A., and Krieger, R. I. (1984). Carbofuran metabolism and toxicity in the rat. *Fundam. Appl. Toxicol.* **4**, 14–21.
- Ferguson, P. W., Jewell, S. A., Krieger, R. I., and Raabe, O. G. (1982). Carbofuran disposition in the rat after aerosol inhalation. *Environ. Toxicol. Chem.* **1**, 245–258.
- Fisher, J. W., Gargas, M. L., Allen, B. C., and Andersen, M. E. (1991). Physiologically based pharmacokinetic modeling with trichloroethylene and its metabolite, trichloroacetic acid, in the rat and mouse. *Toxicol. Appl. Pharmacol.* **109**, 183–195.
- Fisher, J. W., Mahle, D., and Abbas, R. (1998). A human physiologically based pharmacokinetic model for trichloroethylene and its metabolites, trichloroacetic acid and free trichloroethanol. *Toxicol. Appl. Pharmacol.* **152**, 339–359.
- Fisher, J. W., Whittaker, T. A., Taylor, D. H., Clewell, H. J., III, and Andersen, M. E. (1989). Physiologically based pharmacokinetic modeling of the pregnant rat: A multiroute exposure model for trichloroethylene and its metabolite, trichloroacetic acid. *Toxicol. Appl. Pharmacol.* **100**(2), 345–359.
- Food Quality Protection Act (FQPA). (1996). *Public Law 104–170*. Available at: <http://www.epa.gov/pesticides/regulating/laws/fqpa/>. Accessed September 2007.
- Gearhart, J. M., Jepson, G. W., Clewell, H. J., III, Andersen, M. E., and Conolly, R. B. (1990). Physiologically based pharmacokinetic and pharmacodynamic model for the inhibition of acetylcholinesterase by diisopropylfluorophosphate. *Toxicol. Appl. Pharmacol.* **106**, 295–310.
- Herzprung, P., Weil, L., and Niessner, R. (1992). Measurement of bimolecular rate constants  $K_i$  of the cholinesterase inactivation reaction by 55 insecticides and of the influence of various pyridinium oximes on  $K_i$ . *Int. J. Environ. Anal. Chem.* **47**, 181–200.
- Hetnarski, B., and O'Brien, R. D. (1975). Electron-donor and affinity constants and their application to the inhibition of acetylcholinesterase by carbamates. *J. Agric. Food Chem.* **23**, 709–713.
- Ivie, G. W., and Dorough, H. W. (1968). Furadan- $C^{14}$  metabolism in lactating cow. *J. Agric. Food Chem.* **16**, 849–855.
- Keys, D. A., Bruckner, J. V., Muralidhara, S., and Fisher, J. W. (2003). Tissue dosimetry expansion and cross-validation of rat and mouse physiologically based pharmacokinetic models for trichloroethylene. *J. Toxicol. Sci.* **76**(1), 35–50.
- Knaak, J. B., Dary, C. C., Okino, M. S., Power, F. W., Zhang, X., Thompson, C. B., Tornero-Velez, R., and Blancato, J. N. (2007). Parameters for carbamate pesticide QSAR and PBPK/PD models for human risk assessment. *Rev. Environ. Contam. Toxicol.* **193**, 53–210.
- Knaak, J. B., Munger, D. M., McCarthy, J. F., and Satter, L. D. (1970). Metabolism of carbofuran alfalfa residues in the dairy cow. *J. Agric. Food Chem.* **18**, 832–837.
- Marshall, T. C., and Dorough, H. W. (1979). Biliary excretion of carbamate insecticides in the rat. *Pestic. Biochem. Physiol.* **11**, 56–63.
- Metcalf, R. L., Fukuto, T. R., Collins, C., Borck, K., El-Aziz, A., Munoz, R., and Cassil, C. C. (1968). Metabolism of 2,2-dimethyl-2,3-dihydrobenzofuranyl-7-N-methylcarbamate (furan) in plants, insects, and mammals. *J. Agric. Food Chem.* **16**(2), 300–311.
- Okino, M. S., Power, F. W., Tornero-Velez, R., Blancato, J. N., and Dary, C. C. (2005). *Assessment of Carbaryl Exposure Following Turf Application Using a Physiological Based Pharmacokinetic Model*. Available at: <http://www.epa.gov/scipoly/sap/2005/february/day1-2.zip>. Accessed March 2007.
- Padilla, S., Marshall, R. S., Hunter, D. L., and Lowit, A. (2007). Time course of cholinesterase inhibition in adult rats treated acutely with carbaryl, carbofuran, formetanate, methomyl, methiocarb, oxamyl or propoxur. *Toxicol. Appl. Pharmacol.* **219**, 202–209.
- Payne, M. P., and Kenny, L. C. (2002). Comparison of models for the estimation of biological partition coefficients. *J. Toxicol. Environ. Health* **65**, 897–931.
- Poulin, P., and Krishnan, K. (1995). An algorithm for predicting tissue: Blood partition coefficients of organic chemicals from n-octanol: Water partition coefficient data. *J. Toxicol. Environ. Health* **46**(1), 117–129.
- Poulin, P., and Theil, F. P. (2000). A priori prediction of tissue: Plasma partition coefficients of drugs to facilitate the use of physiologically based pharmacokinetic models in drug discovery. *J. Pharm. Sci.* **89**, 16–35.
- Poulin, P., and Theil, F. P. (2002). Prediction of pharmacokinetics prior to *in vivo* studies: 1. Mechanism-based prediction of volume of distribution. *J. Pharm. Sci.* **91**, 129–156.
- Roth, W. L., Freeman, R. A., and Wilson, A. G. (1993). A physiologically based model for gastrointestinal absorption and excretion of chemicals carried by lipids. *Risk Anal.* **13**, 531–543.
- Simmons, J. E., Boyes, W. K., Bushnell, P. J., Raymer, J. H., Limsakun, T., McDonald, A., Sey, Y. M., and Evans, M. V. (2002). A physiologically based pharmacokinetic model for trichloroethylene in the male Long-Evans rat. *J. Toxicol. Sci.* **69**(1), 3–15.
- U.S. Environmental Protection Agency (U.S. EPA). (2004). *Exposure Related Dose Estimating Model (ERDEM) for Assessing Human Exposure and Dose (EPA/600/X-04/060)*. Available at: [http://epa.gov/headweb/erdem/erdem\\_report.pdf](http://epa.gov/headweb/erdem/erdem_report.pdf). Accessed March 2007.
- U.S. Environmental Protection Agency (U.S. EPA). (2005). *Estimation of Cumulative Risk from N-Methyl Carbamate Pesticides: Preliminary Assessment*. U.S. Environmental Protection Agency, Office of Pesticide Programs. Available at: <http://www.epa.gov/scipoly/sap/meetings/2005/august/preliminarynmc.pdf>. Accessed September 2007.
- US Environmental Protection Agency (U.S. EPA). (2006a). *Interim Reregistration Eligibility Decision Carbofuran (EPA-738-R-06-031)*. Available at: [http://www.epa.gov/REDS/carbofuran\\_ired.pdf](http://www.epa.gov/REDS/carbofuran_ired.pdf). Accessed March 2007.
- U.S. Environmental Protection Agency (U.S. EPA). (2006b). *Carbofuran. HED Revised Risk Assessment for the Reregistration Eligibility Decision (RED) document (Phase 4). PC090601. DP#327359*. Available at: <http://www.epa.gov/fedrgstr/EPA-PEST/2006/March/Day-22/p2708.htm>. Accessed September 2007.
- Usmani, K. A., Hodgson, E., and Rose, R. L. (2004). *In vitro* metabolism of carbofuran by human, mouse, and rat cytochrome P450 and interactions with chlorpyrifos, testosterone, and estradiol. *Chem. Biol. Interact.* **150**, 221–232.
- Yu, C., Metcalf, R. L., and Booth, G. M. (1972). Inhibition of acetylcholinesterase from mammals and insects by carbofuran and its related compounds and their toxicities toward these animals. *J. Agric. Food Chem.* **20**(5), 923–926.